



Universiteit
Leiden
The Netherlands

Neuroimaging biomarkers in genetic frontotemporal dementia : towards a timely diagnosis

Feis, R.A.

Citation

Feis, R. A. (2020, October 14). *Neuroimaging biomarkers in genetic frontotemporal dementia : towards a timely diagnosis*. Retrieved from <https://hdl.handle.net/1887/137726>

Version: Publisher's Version

License: [Licence agreement concerning inclusion of doctoral thesis in the Institutional Repository of the University of Leiden](#)

Downloaded from: <https://hdl.handle.net/1887/137726>

Note: To cite this publication please use the final published version (if applicable).

Cover Page



Universiteit Leiden



The handle <http://hdl.handle.net/1887/137726> holds various files of this Leiden University dissertation.

Author: Feis, R.A.

Title: Neuroimaging biomarkers in genetic frontotemporal dementia : towards a timely diagnosis

Issue Date: 2020-10-14



Chapter 6

Frontotemporal dementia vs. Alzheimer's disease: specificity of multimodal MRI in at-risk groups

Published in *BMC Neurology* 2019;19(1):343 as:

Multimodal MRI of grey matter, white matter, and functional connectivity in cognitively healthy mutation carriers at risk for frontotemporal dementia and Alzheimer's disease

Rogier A. Feis, Mark J.R.J. Bouts, Elise G.P. Dopper, Nicola Filippini, Verena Heise, Aaron J. Trachtenberg, John C. van Swieten, Mark A. van Buchem, Jeroen van der Grond, Clare E. Mackay, Serge A.R.B. Rombouts

Abstract

Frontotemporal dementia (FTD) and Alzheimer's disease (AD) are associated with divergent differences in grey matter volume, white matter diffusion, and functional connectivity. However, it is unknown at what disease stage these differences emerge. Here, we investigate whether divergent differences in grey matter volume, white matter diffusion, and functional connectivity are already apparent between cognitively healthy carriers of pathogenic FTD mutations, and cognitively healthy carriers at increased AD risk.

We acquired multimodal magnetic resonance imaging (MRI) brain scans in cognitively healthy subjects with ($n = 39$) and without ($n = 36$) microtubule-associated protein tau (*MAPT*) or progranulin (*GRN*) mutations, and with ($n = 37$) and without ($n = 38$) apolipoprotein E $\epsilon 4$ (*APOE4*) allele. We evaluated grey matter volume using voxel-based morphometry, white matter diffusion using tract-based spatial statistics (TBSS), and region-to-network functional connectivity using dual regression in the default mode network and salience network. We tested for differences between the respective mutation carriers and controls, as well as for divergence of those differences. For the divergence contrast, we additionally performed region-of-interest TBSS analyses in known areas of white matter diffusion differences between FTD and AD (i.e., uncinata fasciculus, forceps minor, and anterior thalamic radiation).

MAPT/GRN mutation carriers did not differ from controls in any modality. *APOE4* carriers had lower fractional anisotropy than controls in the callosal splenium and right inferior fronto-occipital fasciculus, but did not show grey matter volume or functional connectivity differences. We found no divergent differences between both carrier-control contrasts in any modality, even in region-of-interest analyses.

Concluding, we could not find differences suggestive of divergent pathways of underlying FTD and AD pathology in asymptomatic risk mutation carriers. Future studies should focus on asymptomatic mutation carriers that are closer to symptom onset to capture the first specific signs that may differentiate between FTD and AD.

Keywords: microtubule-associated protein tau; progranulin; apolipoprotein E4; voxel-based morphometry; diffusion tensor imaging (DTI); tract-based spatial statistics (TBSS); functional connectivity; dual regression; frontotemporal dementia; Alzheimer's disease

Introduction

Frontotemporal dementia (FTD) and Alzheimer's disease (AD) are two of the most common causes of dementia (Lobo et al., 2000; Plassman et al., 2007; Seelaar et al., 2008; Vieira et al., 2013). In addition to distinct clinical features (Gorno-Tempini et al., 2011; McKhann et al., 2011; Rascovsky et al., 2011; Seelaar et al., 2011; Galimberti & Scarpini, 2012), FTD and AD demonstrate different patterns of functional and structural neurodegeneration on magnetic resonance imaging (MRI; Seeley et al., 2007; Zhang et al., 2009, 2011; Zhou et al., 2010; Mahoney et al., 2014; Möller et al., 2015b; Daianu et al., 2016; Tuovinen et al., 2017). Atrophy is more pronounced in FTD than in AD in frontotemporal areas such as the anterior cingulate cortex, fronto-insula, and inferior frontal cortex (Seeley et al., 2007; Zhang et al., 2011; Möller et al., 2015b). Conversely, AD patients have more atrophy in the occipital gyrus and precuneus than FTD patients (Zhang et al., 2011). In terms of white matter diffusion tensor imaging (DTI) alterations, FTD patients have reduced fractional anisotropy (FA) and increased radial diffusivity (RD) compared to AD patients in the uncinate fasciculi, forceps minor, and anterior thalamic radiation, whereas AD patients do not show FA decreases or RD increases compared to FTD patients (Zhang et al., 2009, 2011; Mahoney et al., 2014; Möller et al., 2015b; Daianu et al., 2016). Furthermore, functional connectivity is inversely affected in FTD and AD. In FTD patients, functional connectivity with the salience network is disrupted, while functional connectivity with the default mode network is increased. Vice versa, functional connectivity with the default mode network is disrupted in AD patients, while functional connectivity with the salience network is increased (Zhou et al., 2010; Tuovinen et al., 2017).

Despite these different patterns of neurodegeneration, the differentiation between FTD and AD is often demanding when patients first present in the memory clinic. For example, FTD patients may present with memory deficits (Graham et al., 2005; Le Ber et al., 2008), and as such may be misdiagnosed as AD patients (Johnson et al., 1999). Conversely, AD patients may be misdiagnosed as FTD patients due to the presentation of behavioural symptoms. Indeed, 13% of initial FTD diagnoses were corrected to AD after two years follow-up (Mendez et al., 2007), while 10–30% of clinical FTD patients were found to have AD pathology upon autopsy (Forman et al., 2006; Knibb et al., 2006; Alladi et al., 2007). The current criteria for behavioural variant FTD (bvFTD; Rascovsky et al., 2011), and language FTD variants (Gorno-Tempini et al., 2011) lack specificity to distinguish early-stage FTD patients from early-stage AD patients (McKhann et al., 2011). This diagnostic problem delays effective disease management (Mohs et al., 2001; Mendez et al., 2007; Mendez, 2009; Pressman & Miller, 2014), and frustrates the development of new treatments. Considering that the potential of disease modifying drugs is highest in the stage before atrophy occurs, the identification of early-stage dementia patients is crucial for patient selection in clinical trials (Rabinovici & Miller, 2010).

To assess whether FTD- and AD-related pathological changes are present even before symptom onset, carriers of FTD and AD risk mutations have been studied using structural, diffusion-weighted, and functional MRI (fMRI). For example, mutations in microtubule-associated protein tau (*MAPT*), progranulin (*GRN*), and repeat expansions in chromosome 9 open reading frame 72 (*C9orf72*) are known causes of genetic FTD. Presymptomatic carriers of these mutations have therefore been regularly studied to investigate early-stage FTD-related pathology (Whitwell et al., 2011a, b; Borroni et al., 2012; Dopper et al., 2014; Pievani et al., 2014). Similarly, mutations in presenilin 1, presenilin 2, and amyloid precursor protein are known causes of genetic AD. However, due to its higher prevalence, apolipoprotein E $\epsilon 4$ (*APOE4*), the strongest risk factor for sporadic AD, has been more extensively used to study early-stage AD-related pathology (Nierenberg et al.,

2005; Cherbuin et al., 2008; Agosta et al., 2009; Filippini et al., 2009, 2011; Honea et al., 2009; Heise et al., 2011; Machulda et al., 2011; Trachtenberg et al., 2012; Matura et al., 2014).

Contrary to findings in clinical FTD and AD (Zhang et al., 2009, 2011; Mahoney et al., 2014; Möller et al., 2015b; Daianu et al., 2016), differences in diffusion metrics associated with asymptomatic *APOE4* (Persson et al., 2006; Gold et al., 2010; Smith et al., 2010; Heise et al., 2011; Adluru et al., 2014; Lyall et al., 2014; Laukka et al., 2015; Cavedo et al., 2017; Operto et al., 2018) are more widespread than diffusion differences associated with asymptomatic *MAPT/GRN* mutation carriers (Dopper et al., 2014; Pievani et al., 2014). Functional connectivity differences have also been shown in these asymptomatic groups (Machulda et al., 2011; Dopper et al., 2014). However, a comparison between these presymptomatic patterns of change in risk mutation carriers for FTD and AD is lacking, even though early-stage differences between these dementias may aid early differential diagnosis.

To this end, we investigated multimodal MRI in asymptomatic subjects at risk for FTD and AD. First, we aimed to replicate early carrier-control differences found between *MAPT/GRN* mutation carriers and controls, and between *APOE4* carriers and controls, respectively, by assessing whole-brain grey matter volume, white matter DTI measures, and functional connectivity in the default mode network and salience network. Secondly, we investigated whether *MAPT/GRN* carrier-control differences diverged from *APOE4* carrier-control differences, similar to FTD-AD differences. For the latter analysis, we additionally evaluated a priori selected white matter tracts known to be affected more strongly in FTD than AD (i.e., uncinate fasciculus, forceps minor, and anterior thalamic radiation). We hypothesised that the differences in grey matter volumes, DTI measures, and functional connectivity seen in FTD and AD patients (Seeley et al., 2007; Zhang et al., 2009, 2011; Zhou et al., 2010; Mahoney et al., 2014; Möller et al., 2015b; Daianu et al., 2016; Tuovinen et al., 2017) may also be present to a smaller extent before symptom onset in risk mutation carriers.

Methods

Participants

Subjects were included retrospectively from studies carried out at the Leiden University Medical Centre (LUMC), The Netherlands, and at the Functional Magnetic Resonance Imaging of the Brain Centre (FMRIB), Oxford, UK.

The Dutch sample included 39 *MAPT/GRN* mutation carriers (11 *MAPT*, 28 *GRN*) and 36 controls, recruited from a pool of 160 healthy first-degree relatives of FTD patients with either *MAPT* or *GRN* mutation (Dopper et al., 2014). Participants were considered asymptomatic in the absence of (1) behavioural, cognitive, or neuropsychiatric change reported by the participant or knowledgeable informant, (2) cognitive disorders on neuropsychiatric tests, (3) motor neuron disease signs on neurologic examination, and (4) other FTD (Gorno-Tempini et al., 2011; Rascovsky et al., 2011) or amyotrophic lateral sclerosis (Ludolph et al., 2015) criteria. Asymptomatic non-carriers from these families and the general population were assumed to have equal risk of developing dementia. *MAPT/GRN* mutation carriers and controls were not tested for *APOE4* alleles.

Data from 37 *APOE4* carriers (30 apolipoprotein E $\epsilon 3/\epsilon 4$ heterozygotes, 7 apolipoprotein E $\epsilon 4/\epsilon 4$ homozygotes) and 38 controls (all apolipoprotein E $\epsilon 3/\epsilon 3$ homozygotes) were collected in Oxford from the general population in Oxfordshire and were selected to match the Dutch sample in terms of age and sex. Due to the limited sample size, it was not possible to match the groups' education level. Middle-aged and elderly *APOE4* carriers and controls underwent a pre-screening cognitive test (Addenbrooke's Cognitive Examination-revised version; Filippini et al., 2011; Heise et al., 2011) to assure asymptomatic status. *APOE4* carriers and controls were not tested for *MAPT/GRN* mutations.

In both cohorts, participants were between 21 and 70 years old. A priori exclusion criteria included MRI contraindications, head injury, current or past neurologic or psychiatric disorders, (history of) substance abuse including alcohol, corticosteroid therapy, type I diabetes therapy, and memory complaints.

The study was conducted in accordance with regional regulations and the Declaration of Helsinki. Written informed consent was received from all participants, and ethical approval for data acquisition was provided by the Medical Ethical Committees in Rotterdam and Leiden for *MAPT/GRN* data, and the National Research Ethics Service Committee South Central—Oxford C for *APOE4* data. For further details regarding the recruitment protocols, see Dopper et al. (2014) for the Dutch sample and Filippini et al. (2011) for the English sample.

Image acquisition

MRI data were acquired with a Philips 3 T Achieva MRI scanner using an 8-channel SENSE head coil (*MAPT/GRN* mutation carriers and controls) or on a Siemens 3 T Trio scanner with a 12-channel head coil (*APOE4* carriers and controls). T_1 -weighted data were acquired with TR = 9.8 ms, TE = 4.6 ms, flip angle = 8°, 140 axial slices, and voxel size = 0.88 × 0.88 × 1.20 mm for *MAPT/GRN* mutation carriers and controls, and using a magnetisation-prepared rapid gradient echo sequence (MPRAGE; TR = 2,040 ms, TE = 4.7 ms, flip angle = 8°, 192 axial slices, voxel size = 1 × 1 × 1 mm) in *APOE4* carriers and controls. Diffusion-weighted images were acquired in 62 directions with TR = 8,250–9,300 ms, TE = 80–94 ms, b-value = 1,000 s/mm², flip angle = 90°, 65–70 axial slices, and voxel size = 2 × 2 × 2 mm. For the resting-state functional MRI (rs-fMRI) scan, subjects were instructed to remain awake and keep their eyes closed (*MAPT/GRN* mutation

carriers and controls) or open (*APOE4* carriers and controls), and to think of nothing in particular. We acquired 180–200 volumes with TR = 2,000–2,200 ms, TE = 28–30 ms, flip angle = 80–89°, and voxel size = 2.75 × 2.75 × 2.75 mm + 10% interslice gap or 3 × 3 × 3.5 mm.

Image analysis

FMRIB Software Library (FSL, <http://www.fmrib.ox.ac.uk/fsl>) tools were used for all data analyses (Jenkinson et al., 2012).

Grey matter volume analyses

Whole-brain voxel-wise structural analysis was carried out with FSL-VBM (Douaud et al., 2007), an optimised voxel-based morphometry protocol (Good et al., 2001) using FSL tools (Smith et al., 2004). First, we performed brain extraction and grey matter segmentation, and registered images to the MNI152 standard space using linear (FLIRT) and nonlinear registration (FNIRT; Anderson et al., 2007). The resulting images were averaged and flipped along the x-axis to create a study-specific grey matter template. Native grey matter images were then re-registered to this template, modulated using the field-warp Jacobian, and smoothed using an isotropic Gaussian kernel with a sigma of 2.5 mm (~ 6 mm full width at half maximum).

Diffusion tensor imaging

Diffusion-weighted imaging scans were processed using FMRIB's Diffusion Toolbox (FDT, <http://www.fmrib.ox.ac.uk/fsl/fdt>). First, we aligned raw diffusion weighted images to the b0-volume using 'eddy correct' to correct for movement and eddy currents. Next, we fitted the diffusion tensor model to the images at each voxel to create modality-specific images for fractional anisotropy (FA), mean diffusivity (MD), axial diffusivity (AxD), and radial diffusivity (RD). For voxel-wise analysis of these images, we used tract-based spatial statistics (TBSS; Smith et al., 2006). After brain extraction, subjects' individual FA images were transformed to standard space using FNIRT. A mean FA image was then created and thinned to generate a whole-brain mean FA skeleton, representing the centres of all white matter tracts common to all subjects. Individual aligned FA images were projected onto this skeleton for group analysis. Similar analyses were performed on MD, AxD, and RD maps using the spatial transformation parameters that were estimated in the FA analysis. For our region-of-interest analyses, we masked the whole-brain skeleton with the combined masks of the uncinate fasciculi, forceps minor, and the bilateral anterior thalamic radiations, which have been shown to differ between FTD and AD patients in terms of DTI metrics (Zhang et al., 2009, 2011; Mahoney et al., 2014; Möller et al., 2015b; Daianu et al., 2016).

Resting-state functional MRI

Prestatistical processing of resting-state data consisted of motion correction (Jenkinson et al., 2002), brain extraction, spatial smoothing using a Gaussian kernel of 6 mm full width at half maximum, 4D grand-mean scaling and high-pass temporal filtering corresponding to a period of 150s (~ 0.007 Hz). Registration to MNI152 standard space was carried out in two steps. We registered echo-planar images onto their respective T₁-weighted structural images using FLIRT and boundary-based registration (Jenkinson & Smith, 2001; Jenkinson et al., 2002; Greve & Fischl, 2009). Next, we used FNIRT to align T₁-weighted structural images to MNI152 standard space, and concatenated the resulting registration matrices to register echo-planar images directly to standard space. Next, we performed individual independent component analysis (ICA) and voxel-wise intensity normalisation (i.e., by dividing all voxels by their time series' mean values and

multiplying by 10,000).

We used FMRIB's ICA-based X-noiseifier (FIX; Griffanti et al., 2014; Salimi-Khorshidi et al., 2014; Feis et al., 2015) to clean up noise components and reduce rs-fMRI scan site bias. For a detailed description and validation of FIX as a multicentre bias reduction method, see Feis et al. (2015). In short, we classified the individual ICA components of a subset of the subjects as signal, noise, or unknown, trained the FIX classifier, and used a leave-one-out test to control the algorithm's quality. All subjects' data were then classified using the optimal threshold (i.e., 20—true-positive rate 95.1%, true-negative rate 91.4%), and structured noise components were removed.

After processing and application of FIX, rs-fMRI data were temporally concatenated and decomposed into 25 components using FSL's group-level ICA tool (Hyvärinen, 1999; Beckmann & Smith, 2004; Beckmann et al., 2005) in order to identify large-scale patterns of functional connectivity. The resulting group-level ICA spatial maps were compared to previously described resting-state networks (Beckmann et al., 2005; Damoiseaux et al., 2006; Rytty et al., 2013; Tian et al., 2013; Bey et al., 2015), and we selected default mode network components and salience network components for dual regression analyses. The default mode network is disrupted in AD and enhanced in FTD, while the salience network is disrupted in FTD and enhanced in AD (Zhou et al., 2010; Tuovinen et al., 2017). Components that included the precuneus, posterior cingulate cortex, angular gyrus, medial prefrontal cortex, and hippocampus were regarded as parts of the default mode network. Components featuring the anterior cingulate cortex, supplementary motor area, and insula were considered linked to the salience network. We found three networks resembling the default mode network (e.g., the anterior, inferior, and posterior default mode network, **Figure 6.1A–C**) and two networks resembling the salience network (e.g., the anterior and posterior salience network, **Figure 6.1D–E**). For these five resulting resting-state networks of interest, we performed dual regression to identify subject-specific spatial maps corresponding to the resting-state networks of interest (Beckmann et al., 2009; Filippini et al., 2009). First, the spatial maps derived from group-level ICA were used as a spatial regressor in each subjects' rs-fMRI data to obtain subject-specific time series describing the temporal dynamics for each component (**Supplemental Figure S6.1**, step 1). Next, the time series found by spatial regression were used as a temporal regressor to find voxels associated with those time series for each subject (**Supplemental Figure S6.1**, step 2). As such, we used the group-level ICA networks of interest to obtain subject-specific spatial maps that allow for voxel-wise comparison. Statistical analysis of region-to-network functional connectivity group differences was then carried out by testing for the functional connectivity between the five resting-state networks of interest and all other grey matter voxels.

Statistical analysis

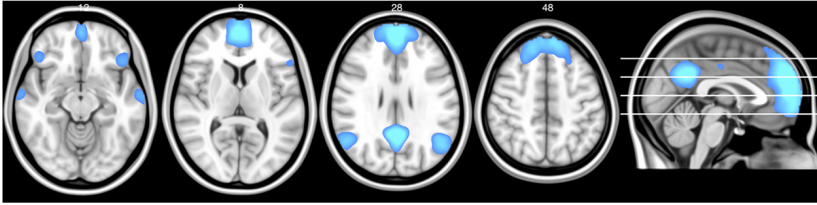
Statistical analysis of grey matter volume, DTI features, and rs-fMRI data was performed using general linear models, including age and education as confound regressors. Additionally, we added a voxel-wise covariate for grey matter volume to the functional connectivity analyses. We tested for differences between *MAPT/GRN* mutation carriers and controls, and for differences between *APOE4* carriers and controls, respectively. Additionally, we tested for the differences between these respective carrier-control contrasts to evaluate whether these gene mutations have divergent effects on the brain in cognitively healthy carriers that might reflect early substrates of FTD or AD pathology. Since possible centre effects are equivalent for carriers and controls at each site, these effects cancel out when we compared the carrier-control effect at one site to the carrier-control effect at the other site. Consequently, unknown confounding factors such as scanner and population differences should have minimal influence on our results.

Pooling *MAPT* and *GRN* mutation carriers, and *APOE4* heterozygotes and homozygotes in our carrier samples may have increased heterogeneity in our groups. To account for this possibility, we performed additional analyses with covariates encoding the difference between *MAPT* and *GRN* mutations, and between *APOE4* hetero- and homozygosity.

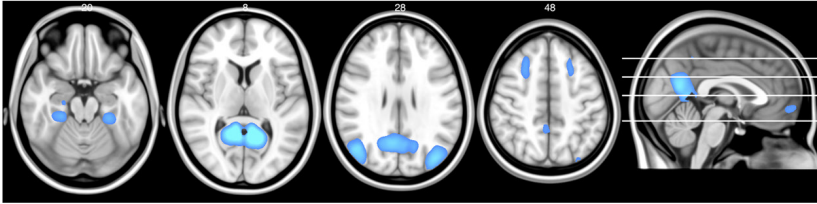
Voxel-wise application of these general linear models to the data was performed using FSL randomise, a permutation-based non-parametric test (5,000 permutations). We set the family-wise error rate at 5% across space by using threshold-free cluster enhancement (Winkler et al., 2014) in all analyses. The alpha level required for statistical significance was set at 0.025 for all imaging analyses, which corresponds to an alpha level of 0.05 in a two-sided *t*-test, since randomise performs the permutation equivalent of a one-sided *t*-test. Minimal cluster size for significant results was set at 10 voxels.

SPSS version 24 (SPSS, Chicago, IL) was used for statistics performed on non-imaging (demographic) variables. Analysis of variance (ANOVA) tests were performed on normally distributed continuous variables (age and education) and included Bonferroni post-hoc tests. A chi-square test was performed for sex. The alpha level required for statistical significance was set at 0.05.

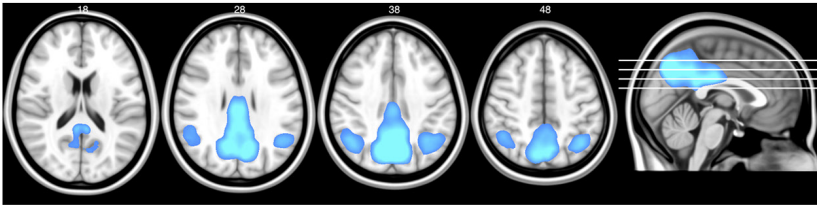
A. Anterior default mode network



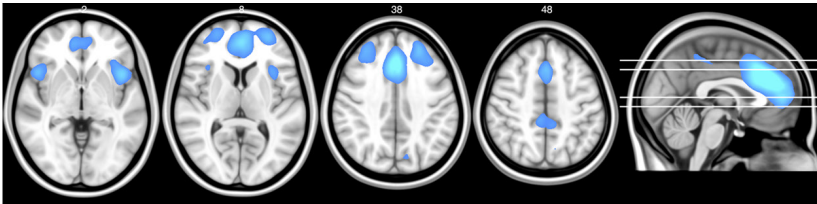
B. Inferior default mode network



C. Posterior default mode network



D. Anterior salience network



E. Posterior salience network

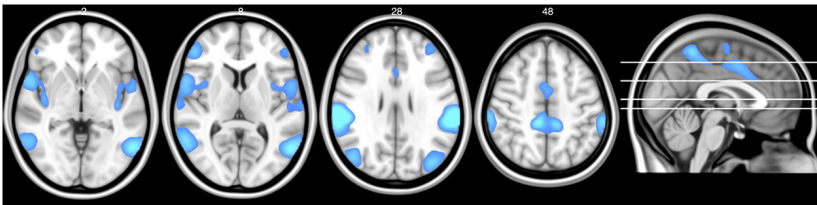


Figure 6.1 Resting-state networks

Maps illustrate the most informative slices of resting-state networks of interest that featured known default mode network and salience network regions and that were used for statistical testing after dual regression.

Results

Demographics

Demographic data for all groups are shown in **Table 6.1**. Age and sex did not differ between groups. Bonferroni post-hoc tests revealed significantly lower education level in years for *MAPT/GRN* mutation carriers than *APOE4* controls ($p = 0.001$), for *MAPT/GRN* controls than *APOE4* controls ($p < 0.001$), and for *MAPT/GRN* controls than *APOE4* carriers ($p = 0.001$).

Table 6.1 Participant demographics

	<i>MAPT/GRN</i>		<i>APOE4</i>		<i>p</i> -value
	Carriers <i>n</i> = 39 ^a	Controls <i>n</i> = 36	Carriers <i>n</i> = 37 ^b	Controls <i>n</i> = 38	
Age, mean (SD) years	50.5 (10.0)	49.8 (11.3)	48.6 (10.3)	50.05 (10.5)	0.86
Sex, <i>n</i> (%) ♀	23 (59%)	18 (50%)	20 (54%)	20 (53%)	0.89
Education, mean (SD) years ^c	14.0 (2.5)	12.6 (2.9)	15.5 (3.7)	16.8 (3.2)	<0.001

APOE4, apolipoprotein E ε4; *GRN*, progranulin; *MAPT*, microtubule-associated protein tau.

^a 11 *MAPT*, 28 *GRN*.

^b 30 heterozygotes, 7 homozygotes.

^c Scores of education level in years were missing for three *MAPT/GRN* mutation carriers and two *MAPT/GRN* controls.

Grey matter volume

We found no grey matter volume differences in *MAPT/GRN* mutation carriers compared to controls, in *APOE4* carriers and compared to controls, nor were there differences between both contrasts.

White matter diffusion

Tract-based spatial statistics revealed no FA, MD, AxD, or RD differences between *MAPT/GRN* mutation carriers and controls. However, we found four clusters of FA reductions in *APOE4* carriers compared to controls (**Table 6.2, Figure 6.2**). Three clusters were located in the forceps major, more specifically in right side of the callosal splenium, and one cluster was located in the right inferior fronto-occipital fasciculus. We found no significant differences between the *MAPT/GRN* and *APOE4* carrier-control contrasts in our whole-brain analysis, nor in our region-of-interest analyses.

Functional connectivity

We found no differences in region-to-network functional connectivity in *MAPT/GRN* mutation carriers compared to controls, in *APOE4* carriers compared to controls, nor between the two carrier-control contrasts in any of the five resting-state networks.

Table 6.2 Cluster information

Cluster	Size	Max t -statistic	MNI coordinates			L/R	Area (peak voxel)
			x	y	z		
1	64	4.14	54	101	72	R	IFOF
2	44	3.19	71	79	95	R	Splenium
3	32	3.58	63	73	87	R	Splenium
4	22	4.19	74	87	98	R	Splenium

Cluster information for significant clusters of reduced FA in *APOE4* carriers compared to controls. Minimum cluster size was 10.

APOE4, apolipoprotein E ϵ 4; FA, fractional anisotropy; IFOF, inferior fronto-occipital fasciculus.

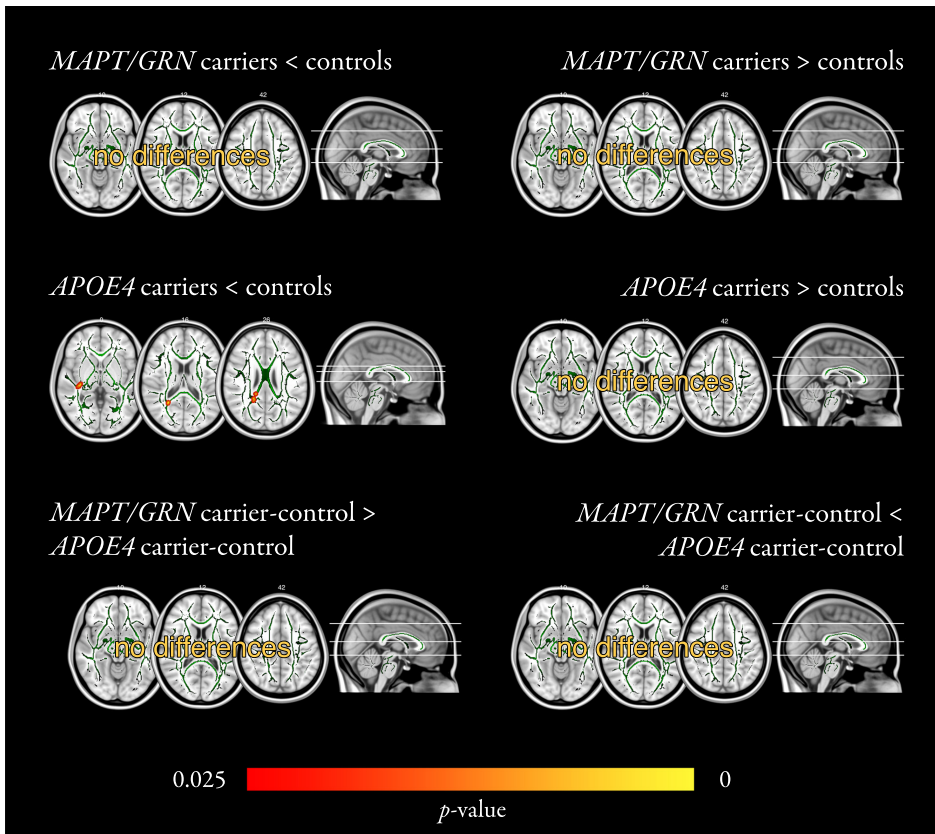


Figure 6.2 White matter FA analysis

Differences in FA (or lack thereof) are shown for each contrast (e.g., *MAPT/GRN* mutation carriers greater or smaller than controls; *APOE4* carriers greater or smaller than controls; *MAPT/GRN* carrier-control differences greater or smaller than *APOE4* carrier-control differences). Mean skeleton maps are shown in green; skeletonised significant results were thickened for better visualisation. Four clusters of FA reductions were found in *APOE4* carriers compared to controls (middle left panel). Colour bar represents significance.

APOE4, apolipoprotein E ϵ 4; FA, fractional anisotropy; *MAPT/GRN*, microtubule-associated protein tau / progranulin.

Heterogeneity analyses

Analyses including covariates for the difference between *MAPT* and *GRN* mutations, and between *APOE4* hetero- and homozygosity yielded results similar to our main analyses. There were no grey matter volume differences between *MAPT/GRN* mutation carriers and controls, *APOE4* carriers and controls, nor between the two carrier-control contrasts. *APOE4* carriers had reduced FA in compared to controls (**Supplemental Figure S6.2**), though only one of the four clusters remained significant. We found no DTI differences between *MAPT/GRN* mutation carriers and controls, nor between the two carrier-control contrasts. We found no differences in region-to-network functional connectivity in *MAPT/GRN* mutation carriers compared to controls, *APOE4* carriers compared to controls, nor between the carrier-control contrasts in any of the five resting-state networks.

Data availability

All non-thresholded statistical images for grey matter volume, white matter diffusion, and functional connectivity results of our default analysis can be found on NeuroVault (Gorgolewski et al., 2015): <https://neurovault.org/collections/NXLXKVCZ/>.

Discussion

Differences in atrophy, white matter diffusion, and functional connectivity patterns have been repeatedly shown between FTD and AD patients (Zhang et al., 2009, 2011; Zhou et al., 2010; Mahoney et al., 2014; Möller et al., 2015b; Daianu et al., 2016), and between asymptomatic mutation carriers at risk for these diseases and controls, e.g., *MAPT* and *GRN* mutation carriers (Whitwell et al., 2011a, b; Borroni et al., 2012; Dopper et al., 2014; Pievani et al., 2014); *APOE4* carriers (Nierenberg et al., 2005; Cherbuin et al., 2008; Agosta et al., 2009; Filippini et al., 2009, 2011; Honea et al., 2009; Heise et al., 2011; Machulda et al., 2011; Trachtenberg et al., 2012; Matura et al., 2014). However, comparisons between groups at risk for FTD and groups at risk for AD have been lacking, even though early-stage differences between these dementias are key to improve on diagnostic standards. In this study, we aimed to replicate previously found differences in asymptomatic mutation carriers at risk for FTD and AD compared to their respective control groups. More importantly, we investigated whether carrier-control differences diverged, similar to the divergences that exist between FTD and AD. While we could replicate some of the previously reported fractional anisotropy reductions in asymptomatic *APOE4* carriers, we found no evidence of divergence between *MAPT/GRN* carrier-control differences and *APOE4* carrier-control differences, even when restricting our DTI analysis to regions which are known to differ between FTD and AD patients. This may suggest that the neuroimaging biomarkers measured in this study are not sufficiently specific to differentiate between FTD-related pathology and pathology possibly related to AD at this early stage.

Our lack of differences between groups in grey matter volume were unsurprising. In asymptomatic risk mutation carriers, one would not expect dementia-related atrophy unless the mutation carrier would be close to symptom onset. Indeed, grey matter volume differences have not been reported in asymptomatic *MAPT/GRN* mutation carriers (Borroni et al., 2012; Dopper et al., 2014), though reports in asymptomatic *APOE4* carriers have been conflicting. While some groups report no grey matter volume differences in asymptomatic *APOE4* carriers (Cherbuin et al., 2008; Filippini et al., 2011; Heise et al., 2011; Matura et al., 2014), others found reduced grey matter volume in the hippocampus (Honea et al., 2009; Cacciaglia et al., 2018), lingual gyrus (Honea et al., 2009), precuneus (Honea et al., 2009; ten Kate et al., 2016), insula (ten Kate et al., 2016), caudate nucleus, precentral gyrus, and cerebellar crus (Cacciaglia et al., 2018). These conflicting findings may in part result from methodological differences, sample sizes, and the different age ranges between studies. Since disease modifying treatments aim to prevent atrophy, one would ideally aim to diagnose dementia patients before atrophy occurs to maximise potential treatment effect. Accordingly, biomarker research should focus on detecting substrates of neurodegeneration that precede atrophy and that may be reversible by future disease modifying treatments.

White matter diffusion analyses yielded areas of reduced FA in *APOE4* carriers compared to controls in the splenium of the corpus callosum, and in the right inferior fronto-occipital fasciculus. These results concur with previous reports in *APOE4* carriers. FA reductions were most often reported in the corpus callosum, cingulum, and inferior fronto-occipital fasciculi (Persson et al., 2006; Gold et al., 2010; Smith et al., 2010; Heise et al., 2011; Adluru et al., 2014; Lyall et al., 2014; Laukka et al., 2015; Cavedo et al., 2017; Operto et al., 2018), while FA differences in the corticospinal tract (Heise et al., 2011; Laukka et al., 2015; Cavedo et al., 2017; Operto et al., 2018) and superior longitudinal fasciculi (Heise et al., 2011; Cavedo et al., 2017; Operto et al., 2018) were less frequently reported. We found no diffusion differences in *MAPT/GRN* mutation carriers compared to controls, in contrast to earlier work (Dopper et al., 2014; Pievani et al., 2014).

However, this might be explained by differences in methodology. One study found significant FA reductions only within certain pre-specified tracts, and, similar to our current study, found no whole-brain differences (Dopper et al., 2014). The other study found differences at $p < 0.005$ uncorrected for multiple comparisons across space. Our analyses were performed with a more restrictive significance level, as we corrected for multiple comparisons across space using threshold-free cluster enhancement, and used the statistical threshold appropriate for a two-sided test, which is not a standard procedure in neuroimaging (Chen et al., 2019). Interestingly, DTI alterations are larger in FTD patients than in AD patients (Zhang et al., 2009, 2011; Mahoney et al., 2014; Möller et al., 2015b; Daianu et al., 2016), while preclinical alterations in *APOE4* carriers (Persson et al., 2006; Gold et al., 2010; Smith et al., 2010; Heise et al., 2011; Adluru et al., 2014; Lyall et al., 2014; Laukka et al., 2015; Cavedo et al., 2017; Operto et al., 2018) are more widespread than in *MAPT/GRN* mutation carriers (Dopper et al., 2014; Pievani et al., 2014). Recently, it has been postulated that white matter DTI differences in genetic FTD develop rather explosively in the years just prior to symptom onset (Feis et al., 2019b; Jiskoot et al., 2019). This might explain why in our sample, we found DTI differences in *APOE4* carriers, but no DTI differences in *MAPT/GRN* mutation carriers. Although there were FA reductions in *APOE4* carriers compared to controls, the difference was not strong enough to result in a difference between the *MAPT/GRN* carrier-control contrast and the *APOE4* carrier-control contrast. We also performed region-of-interest analyses in the uncinate fasciculi, forceps minor, and bilateral anterior thalamic radiations, which were found to have FA reductions and RD increases in FTD patients compared to AD patients (Zhang et al., 2009, 2011; Mahoney et al., 2014; Möller et al., 2015b; Daianu et al., 2016). However, even in these regions of interest, we could not find DTI differences between the *MAPT/GRN* carrier-control contrast and the *APOE4* carrier-control contrast. As such, we could not conclude that *MAPT/GRN* mutation carriership had a different effect on white matter diffusion metrics than *APOE4* carriership.

It has been previously argued that the default mode network and the salience network are inversely correlated and both play a role in AD and FTD. Specifically, functional connectivity in the default mode network was reported to be reduced in AD patients and increased in FTD patients, whereas functional connectivity in the salience network was reported to be inversely affected: reduced in FTD patients and increased in AD patients (Zhou et al., 2010; Tuovinen et al., 2017). In asymptomatic *APOE4* carriers, this inverse correlation was also shown. Functional connectivity with the default mode network was decreased and functional connectivity with the salience network was enhanced in *APOE4* carriers compared to controls (Machulda et al., 2011). In asymptomatic *MAPT* and *GRN* mutation carriers, functional connectivity was reduced in the salience network, but no differences in the default mode network were found (Dopper et al., 2014). Based on these results, we hypothesised that functional connectivity in the default mode network and salience network would be ideal candidates to screen for early changes in asymptomatic risk mutation carriers. However, we found no evidence of functional connectivity differences, either between the respective carrier and control groups or divergent differences between the carrier-control contrasts. This might in part be a power issue but could also be explained by population and methodological differences. For example, our sample was on average younger and had a broader age range than the *APOE4* sample investigated by Machulda et al. (2011). Furthermore, we performed data-driven dual regression analyses, whereas both Machulda et al. (2011) and Dopper et al. (2014) performed seed-based analyses. While small seed areas are arbitrarily placed and may be subject to registration mismatch, dual regression networks are less sensitive to these issues due to their data-driven origin. Indeed, dual regression is amongst the best functional MRI analysis techniques in

terms of test-retest reliability (Zuo et al., 2010; Zuo & Xing, 2014). Therefore, the most likely explanation of our functional connectivity results is that our groups were on average too far from symptom onset for functional connectivity alterations in the default mode network and salience network to robustly appear.

Strengths of this study include its unique design to pick up differences between FTD- and AD-related pathology in asymptomatic populations, and the inclusion of control groups from both sites to deal with potential scan site bias. We performed specific region-of-interest analyses to increase power to find differences in DTI metrics. Furthermore, we used FIX (Griffanti et al., 2014; Salimi-Khorshidi et al., 2014) to clean up structured noise (e.g., motion, artefacts) from rs-fMRI data to reduce scanner-based functional connectivity differences (Feis et al., 2015) and increase the signal-to-noise ratio. To account for possible heterogeneity resulting from pooling *MAPT* and *GRN* mutation carriers, and *APOE4* hetero- and homozygotes, we performed additional analyses including covariates for the different mutation types. The results of these analyses were very similar to our main results, suggesting that the effect of genetic heterogeneity in our main analyses was altogether limited. Limitations must also be considered. Firstly, differences in penetrance and age of onset exist between *MAPT/GRN* and *APOE4*. *MAPT* and *GRN* mutations have an autosomal dominant inheritance pattern, and are highly penetrant (van Swieten et al., 2000; van Swieten & Heutink, 2008). On the other hand, *APOE4* has a dose-dependent effect on lifetime AD risk. Heterozygous *APOE4* carriers have an estimated lifetime risk for AD of approximately 25%, while *APOE4* homozygosity is associated with an estimated lifetime risk of around 55% (Genin et al., 2011). Therefore, it is unlikely that all *APOE4* carriers from our sample will develop AD, which reduced our power to detect AD-related differences. For the same reason, it cannot be entirely ruled out that some of the differences associated with the *APOE4* carriers do not reflect presymptomatic AD-related pathology. Information on *MAPT/GRN* mutation carriership was not available for *APOE4* carriers and controls, and information on *APOE4* carriership was not available for *MAPT/GRN* mutation carriers and controls. Due to the infrequency of *MAPT* and *GRN* mutations, it is unlikely that *APOE4* carriers or controls had an *MAPT* or *GRN* mutation. However, the frequency of the *APOE4* allele in Caucasian populations is around 14% (Eisenberg et al., 2010), and it is likely that some of the *MAPT* and *GRN* mutation carriers and controls had an *APOE4* allele. As *MAPT/GRN* mutation carriers and controls were from the same families, the frequency of the *APOE4* alleles within these groups was most likely similar. Therefore, the effect of *APOE4* on our *MAPT/GRN* analyses is presumably small. The broad age range in our groups presents another limitation. FTD- or AD-related pathology may be absent or present in a lesser degree in young mutation carriers than in older mutation carriers, who are closer to symptom onset. However, even though a broad age range was present in our sample, physiological brain ageing effects are unlikely to have influenced our results. The four groups were matched for age, and age was added as confound covariate to the model. Therefore, physiological brain ageing effects should be equally distributed across groups and were accounted for in the model. In order to increase power, future neuroimaging research comparing FTD- and AD-related pathology in asymptomatic risk groups should contain clinical follow-up and conversion information, which will enable the inclusion of a time to onset variable to the model.

Conclusion

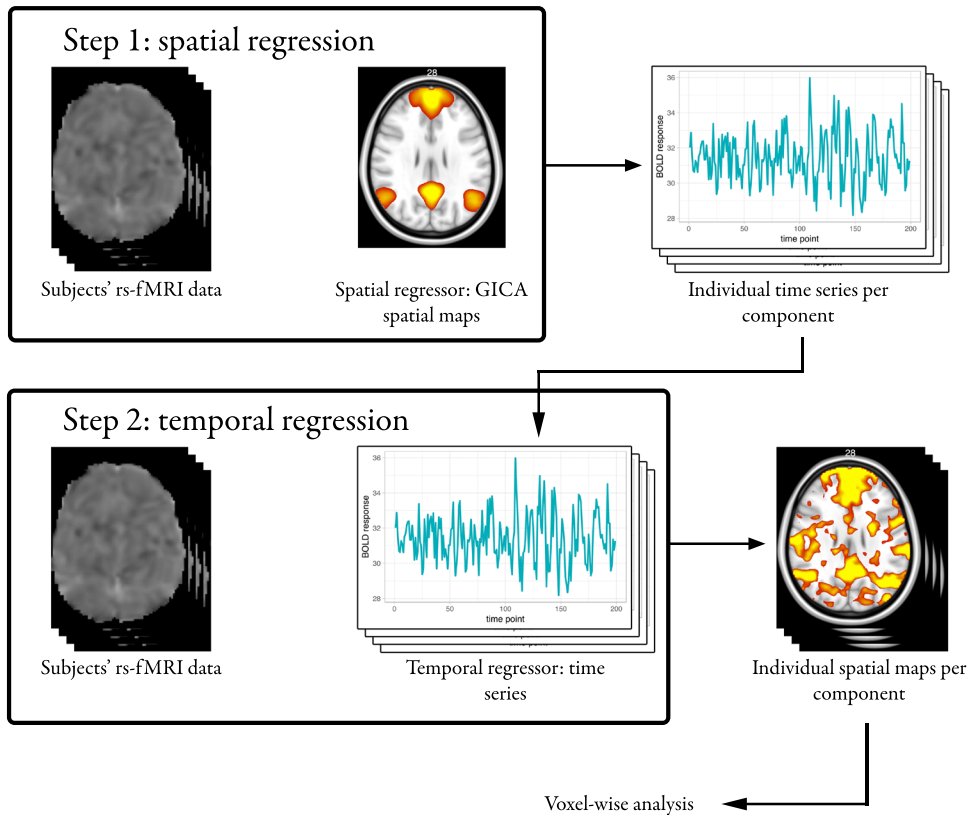
Dementias are relentlessly progressive diseases for which no adequate treatments currently exist, and differentiation between various forms of dementia is clinically challenging. Recently, MRI has shown different patterns of grey matter atrophy, DTI alterations, and functional connectivity differences in

AD and FTD patients (Zhang et al., 2009, 2011; Zhou et al., 2010; Mahoney et al., 2014; Möller et al., 2015b; Daianu et al., 2016; Tuovinen et al., 2017). However, early differential identification of at-risk groups is key to study pathophysiological processes, develop disease modulating drugs and, eventually, identify patient groups that may benefit from these treatments. In the current study, we could not find differences suggestive of divergent pathways of underlying FTD and AD pathology in asymptomatic risk mutation carriers.

Acknowledgements

Our appreciation goes out to all study participants. The authors of this work were supported by the Leiden University Medical Centre MD/PhD Scholarship (to RAF); HDH Wills 1965 charitable trusts (to NF, English Charity Register 1117747); an Alzheimer's Research UK studentship (to VH, English Charity Register 1077089); a Rhodes scholarship (to AJT); ZonMw programme Memorabel project 733050103, JPND PreFrontAls consortium project 733051042 (to JCvS), the National Institute for Health Research (NIHR), UK as part of the Oxford Biomedical Research Centre (BRC; to CEM) and a VICI grant 016-130-667 from The Netherlands Organisation for Scientific Research (NWO; to SARBR). The views expressed are those of the authors and not necessarily those of the NWO, the NHS or the NIHR. The funding sources were not involved in the design of the study; in the collection, analysis and interpretation of data; in the writing of the report; and in the decision to submit the article for publication. The authors report no conflict of interest.

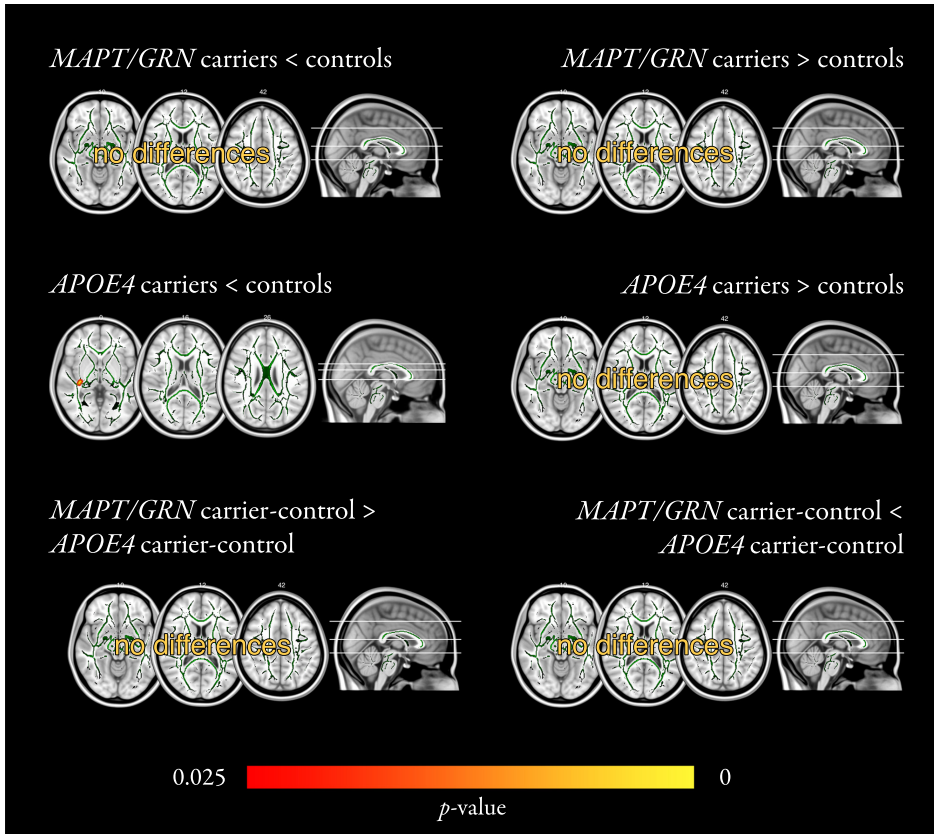
Supplemental material



Supplemental Figure S6.1 Dual regression

Subject-specific spatial maps for statistical testing are acquired from GICA spatial maps in two steps. First, GICA spatial maps are used as spatial regressor on each subject's rs-fMRI data to obtain time series associated with those GICA components (step 1). Next, these time series are used as temporal regressor to obtain subject-specific spatial maps for each component (step 2). These maps are then used for voxel-wise statistical testing.

GICA, group-level independent component analysis; rs-fMRI, resting-state functional magnetic resonance imaging.



Supplemental Figure S6.2 White matter FA analysis with mutation covariates

In this analysis, covariates for the differences between *MAPT* and *GRN* mutations, and between *APOE4* hetero- and homozygosity were added to account for genetic heterogeneity. Differences in FA (or lack thereof) are shown for each contrast (e.g., *MAPT/GRN* mutation carriers greater or smaller than controls; *APOE4* carriers greater or smaller than controls; *MAPT/GRN* carrier-control differences greater or smaller than *APOE4* carrier-control differences). Mean skeleton maps are shown in green; skeletonised significant results were thickened for better visualisation. One cluster of FA reductions was found in *APOE4* carriers compared to controls (middle left panel). Colour bar represents significance.

APOE4, apolipoprotein E ε4; FA, fractional anisotropy; *MAPT/GRN*, microtubule-associated protein tau / progranulin.